

Overlap Removal of Dimensionality Reduction Scatterplot Layouts

Gladys M. Hilaraca, Wilson E. Marcílio-Jr, Danilo M. Eler, Rafael M. Martins, and Fernando V. Paulovich, *Member, IEEE*

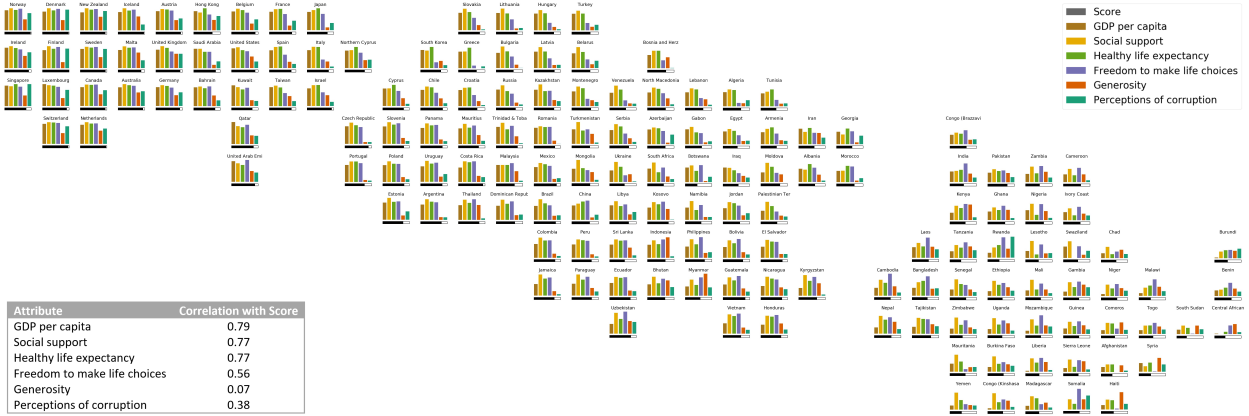


Fig. 1. DGrid overlap-free layout of a projection from the World Happiness Report 2019 data [21]. Visual markers encode the perceived happiness as horizontal black bars and other indicators using a bar chart. As in the original DR scatterplot, three big groups of countries are observed, reflecting the perceived happiness score. However, in this overlap-free representation, not only inter-group analysis is readily supported but also intra-group, allowing detailed examination of individual instances and existing patterns, which helps users take full advantage of DR layouts.

Abstract—Dimensionality Reduction (DR) scatterplot layouts have become a ubiquitous visualization tool for analyzing multidimensional data items with presence in different areas. Despite its popularity, scatterplots suffer from occlusion, especially when markers convey information, making it troublesome for users to estimate items' groups' sizes and, more importantly, potentially obfuscating critical items for the analysis under execution. Different strategies have been devised to address this issue, either producing overlap-free layouts, lacking the powerful capabilities of contemporary DR techniques in uncover interesting data patterns, or eliminating overlaps as a post-processing strategy. Despite the good results of post-processing techniques, the best methods typically expand or distort the scatterplot area, thus reducing markers' size (sometimes) to unreadable dimensions, defeating the purpose of removing overlaps. This paper presents a novel post-processing strategy to remove DR layouts' overlaps that faithfully preserves the original layout's characteristics and markers' sizes. We show that the proposed strategy surpasses the state-of-the-art in overlap removal through an extensive comparative evaluation considering multiple different metrics while it is 2 or 3 orders of magnitude faster for large datasets

Index Terms—Dimensionality reduction, Multidimensional Projection, Scatterplots, Overlap removal

1 INTRODUCTION

Scatterplots are among the most prevalent visualizations in exploratory data analysis [31, 43, 52]. Despite their popularity, they suffer from the same issue present in most 3D (we love to hate) visual representations: occlusion [3]. As the overlap between points or markers increases, scatterplots become less effective [43, 44, 52], affecting our comprehension [26] and the correctness of analytical tasks, since non-visible objects are prone to be ignored [13]. Even simple design choices, like markers' rendering order [31], can result in misleading layouts, and the problem is amplified when the markers convey complex information, such as images [12] or icons [6], occupying more space.

For the general case, different strategies have been proposed to tackle this problem, including sampling, abstraction, re-sizing, changing opacity, and a combination of those [52]. Despite the differences, the underlying idea is to transform a scatterplot so that typical tasks of correlation estimation, class separation, outlier detection, distribution detection, and point value reading [31] are still valid. For the particular case of Dimensionality Reduction (DR) visualization [35]—the most accepted approach for high-dimensional data in visual analytics [42, 44]—this list can be relaxed. Since exact positions in the axes are not relevant, and the critical information is distance and neighbor-

hood relationships, correlation estimation and point-value reading are pointless. This opens the possibility of rearranging the layout, changing the points' coordinates to remove overlaps.

In the literature, many solutions can be found to address this problem. Some techniques that seek to create DR scatterplots without overlap [36, 37] lack the powerful capabilities of contemporary DR techniques in uncovering interesting data patterns. Post-processing techniques that remove overlaps of any given scatterplot focus on rearranging scatterplots by moving markers while maintaining, as much as possible, the characteristics of the original scatterplot. Optimization of cost functions has been used in this process [16, 19], with the inherent problems of numerical stability of such solutions. Orthogonal scan-line-based algorithms are also common [11, 17, 20, 32], usually delivering better results. In general, the existing solutions have problems to preserve different scatterplots' characteristics at the same time, usually favoring some aspects to the detriment of others. Also, resulting layouts are typically distorted, often resulting in markers of unreadable dimensions, defeating the purposes of overlap removal.

This paper presents *Distance Grid (DGrid)*, a novel approach for overlap removal of DR scatterplots that combines a density-based strategy to generate auxiliary points with a novel space-partitioning method. DGrid is fast and renders a good compromise between the preservation of different scatterplots' characteristics. Compared to seven state-of-the-art techniques, DGrid presents the best trade-off regarding multiple aspects while producing low distortions and preserving the

same dimensions of the input layouts, consistently resulting in visual representations with readable markers. Also, in a user study with 42 participants, DGrid was selected as the best technique in preserving the general appearance of original scatterplots while rendering aesthetically pleasant layouts.

In summary, the main contributions of this paper are:

- A novel, fast, and highly precise method for overlap-removal of DR scatterplots that presents a good trade-off between different aspects of layout preservation;
- A thorough analysis of the literature to better formalize the problem of scatterplot characteristics' preservation, consolidating a set of concepts and metrics;
- An extensive comparative analysis of overlap removal techniques involving seven state-of-the-art approaches plus our proposed one.

2 RELATED WORK

In the literature, when scatterplots are used to represent Dimensionality Reduction (DR) layouts, the two most common strategies to address occlusion while maintaining all visual markers are: (1) creating overlap-free layouts from scratch; or (2) eliminating overlaps as a post-processing strategy. Some techniques have been proposed in the former group, for instance, IncBoard [37] and HexBoard [36]. Although interesting solutions, they lack the powerful capabilities of contemporary DR techniques to uncover meaningful data patterns. In the latter, some methods remove overlaps by mapping scatterplot points into orthogonal grid cells preserving distances, such as IsoMatch [15], Kernelized Sorting [38], and NMAP [10]. However, grid approaches negatively affect important analytical tasks such as class separation, outlier, and distribution detection [31], since all empty space is removed and gaps are usually beneficial [30]. It is also possible to create distance-preserving grids without considering DR layouts as inputs [1, 14, 28, 39, 46, 47, 50], but they are out of our scope.

Aiming to preserve empty spaces while promoting overlap removal, a group of techniques heuristically rearrange layouts by moving visual markers, maintaining, as much as possible, the characteristics of a given scatterplot [8, 25]. This paper focuses on discussing the problem when the scatterplot presents rectangular markers, so we refrain from discussing other potential shapes, for instance, diamonds [7, 29].

RWordle [45] is one example of overlap-removal technique for rectangular markers. It replaces markers searching empty positions in spiral movements, and contains two variants that differ on the ordering the points are processed: RWordle-L orders visual markers along a scan-line, while RWordle-C orders them using distances. RWordle is not precise in preserving essential characteristics of the original layout, such as the similarity relationships among visual markers [25]. It also results in unreasonable running time for dense scatterplots, causes excessive displacement of markers, and loss of distance relations.

ProjSnippet [19] focuses specifically on distance preservation by maximizing an energy function that accounts for similarity preservation and overlap removal. It presents limitations when the original scatterplot has groups of points with high-density. In these cases, the technique uses too much space to reduce overlap while preserving the similarity among points, often distorting and creating overlap-free layouts with unreadable markers, defeating the purpose of removing overlaps. One problem with ProjSnippet is the optimization procedure that, in some cases, suffers from numerical instability. Another technique, called MIOLA [18], uses mixed-integer quadratic programming to rearrange rectangular boxes in the visual space. MIOLA usually presents more compact layouts after overlap removal. However, it does not preserve well orthogonal ordering and neighborhoods [18].

Another technique that relies on optimization is PRISM [16]. PRISM creates a proximity graph on top of the original layout using triangulation, then minimizes a stress function considering an overlap factor between each pair of nodes in the graph. Scatterplot density also affects its running time, and it suffers from similar problems with optimization instability, sometimes resulting in layouts that are not overlap-free. Triangulation is also used in the GTree method [34], with the triangulation edges used to define a cost function that builds a minimum

cost spanning tree. GTree interactively grows the edges' length of such tree until there are no more overlaps. It maintains the global shape but excessively moves visual markers, requiring too much space for the final layout, considerably reducing markers size [8].

A well-explored strategy to reduce overlap is to process the x and y axes individually. The Push Force-Scan (PFS) [32] is one of the pioneers. PFS orders rectangles in the horizontal/vertical direction and applies the minimum movement to remove overlap among subsequent visual markers, focusing on orthogonal ordering preservation. PFS tends to displace markers considerably, not preserving the initial layout's global shape [8], and adds unnecessary spaces between markers. To reduce such spaces, PFS' [20] moves markers horizontally/vertically based on the maximum movement distance from previous markers, unlike the sum of previous markers as PFS. The overlap-free layout is improved, but it still presents unnecessary spread and may not maintain the input layout's global shape. Another technique that treats each axis separately is VPSC [11]. It defines non-overlap constraints for the x and y axes, related to how much a visual marker needs to be moved in the corresponding direction. As with the previous techniques, for scatterplots presenting dense groups of points, the resulting layouts diverge from the original layouts. ReArrange [17] considers pairs of overlapping nodes, one by one, resolving the occlusion problem with the smallest displacement possible while preserving orthogonal order. Like in VPSC, ReArrange finds overlaps among visual markers using a line-sweep algorithm and applies overlap removal on x and y axes separately. ReArrange is one of the best performing approaches to date, but it distorts the original layout's global shape and increases the layout dimensions, reducing markers size.

In our technique, global shape preservation and spread are explicitly controlled, producing overlap-free layouts with low distortions and the same dimensions as the original layouts, and resulting in visualizations with readable markers (if they are legible on the original scatterplot). Also, without negatively affecting running time, distance and neighborhood relationships are precisely maintained, an essential aspect since many DR analytical tasks are focused on that.

3 METHOD

3.1 Problem Formulation and Design Guidelines

In general terms, the problem we are solving is, given a scatterplot \mathcal{P} composed of N points or visual markers $\mathcal{P} = \{p_1, \dots, p_N\} \in \mathbb{R}^2$, where (x_i, y_i) are the top-left corner coordinates of p_i with (w_i, h_i) its dimensions, create a new scatterplot $\mathcal{P}' = \{p'_1, \dots, p'_N\} \in \mathbb{R}^2$ where the markers' overlaps are removed and the overall structure of \mathcal{P} is preserved as much as possible. Based on the current literature, structure preservation can be defined and measured through a set of different principles and metrics. Here, we transform them into design guidelines for the general problem of overlap removal in Dimensionality Reduction (DR) scatterplots.

DG1 – Remove markers' overlaps. The resulting scatterplot \mathcal{P}' should present minimum overlap among markers, eliminating occlusions that may hide important information. To measure occlusion, we average the pairwise *overlap coefficient* [40] among all graphical markers, computing

$$overlap = \sqrt{\frac{1}{N(N-1)} \sum_i \sum_{j \neq i} \frac{\mathcal{A}(p_i \cap p_j)}{\min\{\mathcal{A}(p_i), \mathcal{A}(p_j)\}}}, \quad (1)$$

where $\mathcal{A}(p_i)$ denotes the area of marker p_i , and the operator \cap returns the intersection of two markers. The overlap coefficient ranges in $[0, 1]$ with 0 indicating an overlap free layout.

DG2 – Preserve markers' global and local distances. Given the typical application of DR layouts for interpreting distance and neighborhood relationships, the overlap-free layout \mathcal{P}' should preserve as much as possible the global distances between markers and local neighborhoods presented in the original scatterplot \mathcal{P} . To measure the global preservation, we use *stress* [23], given by

$$stress = \sqrt{\frac{\sum_i^N \sum_j^N (||p_i - p_j|| - ||p'_i - p'_j||)^2}{\sum_i^N ||p_i - p_j||^2}}. \quad (2)$$

Stress ranges in $[0, +\infty[$ with 0 indicating perfect preservation of distances. Notice that to reduce distortions, the transformed layout \mathcal{P}' should be scale to the same dimensions of the original layout \mathcal{P} . To measure the local neighborhood preservation, we use *trustworthiness* [48], given by

$$trustworthiness = 1 - \frac{2}{NK(2N-3K-1)} \sum_i^N \sum_{j \in U_K^i} (r(i, j) - K), \quad (3)$$

where U_K^i is the set of points that are in the neighborhood of size K of $p'_i \in \mathcal{P}'$ but not in neighborhood of size K of $p_i \in \mathcal{P}$, and $r(i, j)$ is the rank of points p_j in the ordering according to the distance from p_i in the original scatterplot. Trustworthiness ranges in $[0, 1]$ with 1 indicating a perfect preservation of the local neighborhoods.

DG3 – Preserve markers' relative positions. An overlap-free layout \mathcal{P}' should not only preserve distances but also relative positions among markers. That is, if p_i is at left/right above/below of p_j , the same ordering should be observed in p'_i and p'_j . This is usually referred to as user mental map preservation and is measured using *orthogonal ordering* [33], given by

$$ordering = \frac{1}{N(N-1)} \left(\sum_{i,j}^N \begin{cases} 1, & \text{if } x_i > x_j \wedge x'_i < x'_j + \\ 0, & \text{otherwise} \end{cases} + \sum_{i,j}^N \begin{cases} 1, & \text{if } y_i > y_j \wedge y'_i < y'_j + \\ 0, & \text{otherwise} \end{cases} \right). \quad (4)$$

The orthogonal ordering ranges in $[0, 1]$, with 0 indicating perfect order preservation.

DG4 – Minimize markers' displacement. The translations applied to the markers to remove the overlaps and create \mathcal{P}' should be as small as possible to preserve the general appearance of \mathcal{P} [33]. To measure this, we use the average displacement [49], given by

$$displacement = \frac{1}{N \sqrt{W'_{bb} * H'_{bb}}} \sum_i^N ||p_i - p'_i||, \quad (5)$$

where W'_{bb} and H'_{bb} are the width and height of \mathcal{P}' bounding box, calculated using

$$\begin{aligned} W_{bb} &= |\max_{i \leq N} (x_i + w_i) - \min_{j \leq N} x_j| \\ H_{bb} &= |\max_{i \leq N} (y_i + h_i) - \min_{j \leq N} y_j| \end{aligned} \quad (6)$$

The *displacement* ranges in $[0, 1]$, with 0 indicating no changes in markers' positions. Notice that the center of both \mathcal{P} and \mathcal{P}' should be translated to the origin to better capture the relative movement [9].

DG5 – Control markers' minimum size. The area occupied by the overlap-free representation should be limited to controlling the displayed markers' minimum size, avoiding creating unreadable markers and resulting in large areas without markers [9]. Visual representations with markers that cannot be read defeat the general purpose of increasing layouts readability by removing overlaps. To quantify this, *layout spread* [33] can be measured using

$$spread = \frac{W'_{bb} \times H'_{bb}}{W_{bb} \times H_{bb}}, \quad (7)$$

where W_{bb} and H_{bb} are the original scatterplot bounding box dimensions calculated using Eq. (6).

DG6 – Preserve global shape. Finally, the overlap-free representation should preserve the original scatterplot's shape, reducing distortions. The usual metric to estimate distortion is the preservation of *aspect-ratio* [9], given by

$$aspect = \max \left(\frac{W'_{bb} \times H_{bb}}{H'_{bb} \times W_{bb}}, \frac{H'_{bb} \times W_{bb}}{W'_{bb} \times H_{bb}} \right). \quad (8)$$

The aspect-ratio metric ranges in $[1, +\infty[$ with 1 the target value.

3.2 Distance Grid (DGrid)

3.2.1 Overview

The trivial solution to the overlap removal problem is to round the (continuous) scatterplot markers' coordinates to the smallest integer range that removes all overlaps. That would satisfy **DG1** (remove overlaps), **DG2** (preserve distances), **DG3** (orthogonal ordering), and **DG6** (preserve global shape). However, it fails on **DG4** (displacement) and **DG5** (minimum marker size) since, for dense scatterplots, the integer range can be quite large, resulting in substantial amounts of empty spaces and tiny unreadable markers. With that in mind, we present *Distance Grid (DGrid)*, a new solution based on grid assignment where empty spaces can be explicitly controlled, accurately fulfilling **DG1**, **DG4**, and **DG5**, while attaining good results for the other guidelines as well. DGrid has four steps (see Fig. 2). In the first, an orthogonal grid \mathcal{G} is superimposed to the scatterplot area with cells sizes equal to the dimensions of the largest marker in \mathcal{P} , and with the number of rows and columns defined by the original scatterplot dimensions (bounding box) **A**. After that, "dummy" points are carefully added to the original scatterplot \mathcal{P} to represent the empty space **B**, and the original and "dummy" points are assigned to individual grid cells using a grid assignment process that minimizes displacement **C**. Finally, the "dummy" points are removed, resulting in a complete overlap-free layout **D**.

3.2.2 Generating the Grid and Adding Dummy Points

Generating the orthogonal grid \mathcal{G} is straightforward. To limit markers' minimum sizes (**DG5**), the cell dimensions are set to (w_{max}, h_{max}) where w_{max} and h_{max} are the maximum width and height among all markers. Also, to preserve the global shape (**DG6**), \mathcal{G} width and height is set to be the same of the original scatterplot \mathcal{P} , so that the number of columns of \mathcal{G} is calculated using $C = W_{bb}/w_{max}$ and the number of rows using $R = H_{bb}/h_{max}$.

As previously explained, once \mathcal{G} is created, "dummy" points are assigned to its cells to represent empty spaces aiming at preserving the general appearance of the original scatterplot, that is, the existing groups, frontiers between groups, and outliers. The idea is to add the "dummy" points in low-density regions but close to original points p_i . In this way, markers' displacement is reduced (**DG3**), since the potential movement of original points is reduced (later discussed in Sec. 3.2.3), and the represented empty spaces focus on the characteristics of the existing groups of points as much as possible since they are close or within those groups (borders).

In this process, we first define a list of candidate "dummy" points $\mathcal{D} = \{d_1, d_2, \dots\} \in \mathbb{R}^2$, generating a point per each cell $g_i \in \mathcal{G}$ that is not occupied by any original point. From this list, since original points will occupy N cells, we select $(R \times C) - N$ points placed in low-density regions. To calculate the region density of a point d_i , we first count the number of original points lying inside each cell, defining $\mathbf{G}_{R \times C}$, then we convolve a Gaussian kernel of size $M \times M$ with \mathbf{G} setting d_i to its center, where M is calculated as

$$M = \frac{W_{BB} \times H_{BB}}{\sum_i^N (w_i \times h_i)}, \quad (9)$$

and kernel's $\sigma = (M - 1)/6$ (notice that M is rounded to the closest larger odd number). In this way, the kernel size is proportional to the

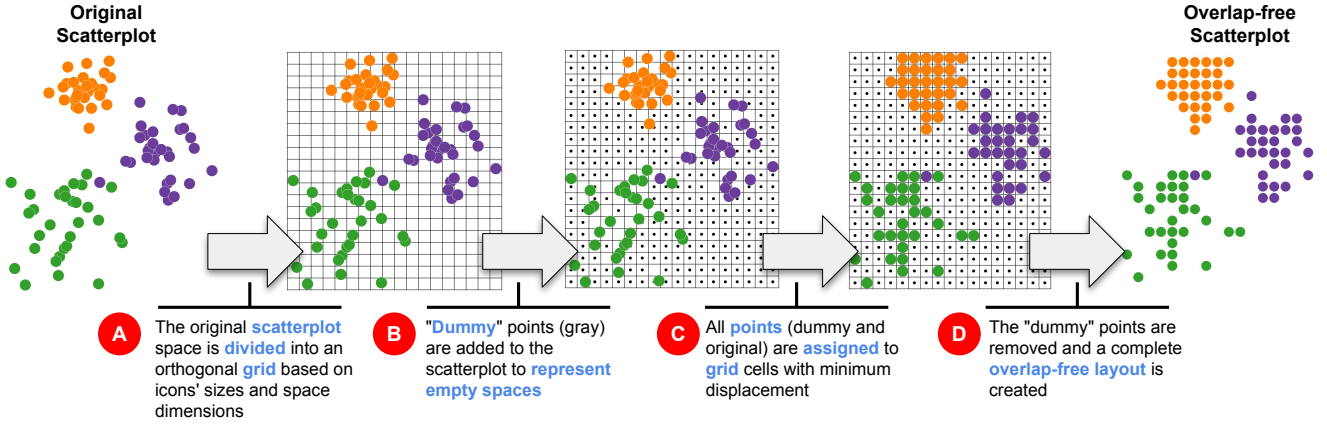


Fig. 2. Overview of DGrid process. The scatterplot area is first split into a grid (A), and “dummy” points (small black dots) are crafted to represent empty space (B). Finally, original and “dummy” points are assigned to grid cells (C), and the “dummy” points are removed (D), resulting in a completely overlap-free layout.

level of details allowed in the overlap-free layout, which is proportional to the number of empty cells per occupied cell, and it smoothly covers the region. Also we zero-padded \mathbf{G} adding $M/2$ rows and columns to its top/bottom and left/right, respectively.

Algorithm 1 Creating “dummy” points.

Input:

- $\mathcal{P} = \{p_1, p_2, \dots, p_N\}$ \triangleright Original Scatterplot
- W_{bb}, H_{bb} \triangleright Bounding box of \mathcal{P} (Eq.(6))
- w_{max}, h_{max} \triangleright Max marker width/height in \mathcal{P}
- $x_{min}, x_{max}, y_{min}, y_{max}$ \triangleright Max/min marker coordinates in \mathcal{P}
- $C \leftarrow \lfloor W_{bb}/w_{max} \rfloor$ \triangleright Calculate the grid number of columns
- $R \leftarrow \lfloor H_{bb}/h_{max} \rfloor$ \triangleright Calculate the grid number of rows

Output:

- $\mathcal{D} = \{d_1, \dots, d_{(R \times C) - N}\}$ \triangleright “Dummy” points

function DUMMY(\mathcal{P}, C, R)

$\mathbf{G}_{R \times C} \leftarrow \text{COUNT}(\mathcal{P}, C, R)$ \triangleright Count the number of points per cell

$\mathbf{K}_{M \times M} \leftarrow \text{MASK}(\mathcal{P})$ \triangleright Calculate an $M \times M$ kernel (Eq.(9))

for $r < R$ **do**

$y \leftarrow r \times (y_{max} - y_{min}) / (R - 1) + y_{min}$

for $c < C$ **do**

if $g_{r,c} = 0$ **then** \triangleright Grid cell is empty

$x \leftarrow c \times (x_{max} - x_{min}) / (C - 1) + x_{min}$

$\delta \leftarrow \sum_i^M \sum_j^M k_{i,j} \times g_{\lfloor r - (M/2) + j \rfloor, \lfloor c - (M/2) + i \rfloor}$

$\mathcal{D} \leftarrow \mathcal{D} \cup (x, y, \delta)$ \triangleright Add candidate “dummy” point

end if

end for

end for

return $\text{FILTER}(\mathcal{D}, (R \times C) - N)$

end function

If different candidate “dummy” points present the same density and we need to choose some of them for the final $(R \times C) - N$ list, we select the closest to any original point. Algorithm 1 details the process of creating the “dummy” points. In this algorithm, function $\text{COUNT}(\mathcal{P}, C, R)$ returns a grid $\mathbf{G}_{R \times C}$ with the number of original points per grid cell, $\text{MASK}(\mathcal{P})$ return the Gaussian kernel of size $M \times M$, and $\text{FILTER}(\mathcal{D}, (R \times C) - N)$ return a list of $(R \times C) - N$ “dummy” points placed in low-density regions close to original points.

Notice that we need to have more cells $R \times C$ than original points N for this approach to work, in other words, $M \geq 1$ (Eq. (9)). If this is not the case, one possibility is to increase grid’s dimensions by a factor $\Delta > 1$, that is, setting $R = \lfloor \Delta \times H_{bb}/h_{max} \rfloor$ and $C = \lfloor \Delta \times W_{bb}/w_{max} \rfloor$. This preserves the global shape (DG6) of the overlap-free layout, but

reduces the markers size, potentially violating DG5. In this paper we did not used this expedient, but it may be useful in practice if Δ is not much larger than one.

3.2.3 Grid Assignment

The last step in our process is to assign each point $c_i \in \mathcal{C} = \mathcal{P} \cup \mathcal{D}$ (complete set of original and “dummy” points) to an individual grid cell $g_i \in \mathcal{G}$ position. For a target grid \mathcal{G} of dimension (R, C) (rows and columns), this process is rather trivial if the marginal distribution of the points’ x -coordinates is perfectly uniform (zero standard deviation) considering a histogram with C bins, and the marginal distribution of the y -coordinates is also perfectly uniform but considering a histogram with R bins. If such distribution holds, the points are very close to the center of individual grid cells, and the displacement to assign them is minimum (DG2 and DG4). In practice, however, this only holds for overlap-free layouts (or very close to that).

Based on this observation, we devise a new algorithm that recursively bisects \mathcal{C} into non-overlapping partitions until the obtained partitions individually present perfectly marginal uniform distributions. Then each partition is assigned to a (sub)grid derived from \mathcal{G} . The spatial partitioning strategy we use is similar to k-d trees [2] but, instead of only considering point positions to segment the space, it incorporates the grid restriction and translates points to grid cells. Given such constraint, we have $R - 1$ different options for horizontal splits and $C - 1$ for vertical splits for the first bisection. So the question is how to select the best bisection, or the sequence of horizontal and vertical bisections, that produces the largest partitions with uniform marginal distributions. This is an impractical combinatorial problem to solve. Instead, we split \mathcal{C} approximately in half in the direction (vertical or horizontal) with more rows or columns. In this way, without any expensive test, we increase our probability of getting the largest partitions with marginal uniform distributions – if the number of points in one partition decreases, this probability increases. However, reducing such probability for the other partition. Therefore half is a natural trade-off.

Thereby, in our process, if $R > C$, we split \mathcal{C} horizontally, obtaining two partitions $\mathcal{C} = \mathcal{C}_1 \cup \mathcal{C}_2$, so that the top partition \mathcal{C}_1 contains enough points to fill (approximately) half of the target grid, that is, $|\mathcal{C}_1| = \lfloor R/2 \rfloor \times C$. Otherwise, we split \mathcal{C} vertically, so that the left partition \mathcal{C}_1 contains enough points to fill (approximately) half of the target grid, that is, $|\mathcal{C}_1| = R \times \lfloor C/2 \rfloor$. This bisecting process is recursively applied to the resulting partitions until obtaining partitions with marginal uniform distribution. In fact, for partitions with perfect uniform marginal distributions, this bisecting process results in the minimum displacement explained at the beginning of this section. Therefore, instead of penalizing our approach’s running time by adding the uniform constraint test, we execute the bisecting process until each

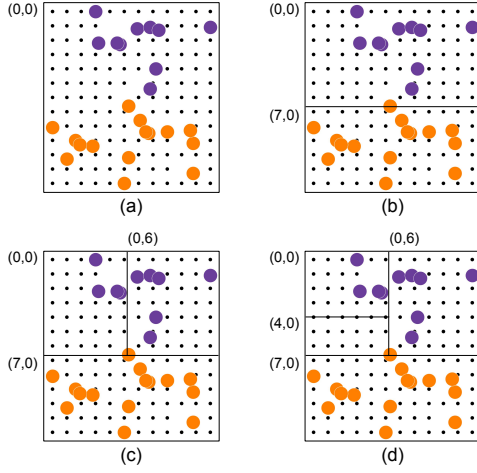


Fig. 3. Process of assigning points to grid cells. In this example, a scatterplot with 156 “dummy” and original points (a) is assigned to a grid with 13 rows and 12 columns. Starting from a horizontal bisection (b), the scatterplot is recursively split until each partition contains only one point, resulting in the grid cell indexes.

partition contains only one instance, rendering a much faster and simpler process to implement.

The last piece to discuss is how to calculate the grid cell indexes (positions) to which the points in \mathcal{C} are assigned. Without loss of generality, if the first bisection vertically splits $\mathcal{C} = \mathcal{C}_1 \cup \mathcal{C}_2$, so that $|\mathcal{C}_1| = R \times \lceil C/2 \rceil$, by construction, the index of the most-left column to which points in \mathcal{C}_1 will be assigned is 0, and the index of the most-left column to which points in \mathcal{C}_2 will be assigned is $\lceil C/2 \rceil$. Similarly, for a horizontal split, the index of the most-top row to which points in \mathcal{C}_1 will be assigned is 0, and the index of the most-top row to which points in \mathcal{C}_2 will be assigned is $\lceil R/2 \rceil$. In the general case, when an input partition is assigned to a grid with R' rows and S' columns, if (i, j) is the index of the top-left corner cell of the input grid, the index of the top-left corner cell to which points in \mathcal{C}_1 will be assigned is (i, j) , and the index of the top-left corner cell to which points in \mathcal{C}_2 will be assigned is $(i + \lceil R'/2 \rceil, j)$ for a horizontal cut, and $(i, j + \lceil C'/2 \rceil)$ for a vertical cut. If the input partition has only one point, (i, j) is the cell index to which the single point is assigned.

Fig. 3 outlines this process. In this example, a scatterplot with 25 original points and 131 “dummy” points (small black dots) is assigned to a grid with $R = 13$ rows and $C = 12$ columns. To start this process, we set the top-left corner cell index to $(0, 0)$ (Fig. 3(a)). Since the input grid has more rows than columns, the first bisection is horizontal (Fig. 3(b)). The resulting top partition contains (approximately) half of the rows (7), and the top-left corner cell of the resulting (sub)grid receives the index $(0, 0)$. The bottom partition contains the remaining rows (6), and the top-left corner cell receives the index $(7, 0)$. Next, the top partition is bisected (Fig. 3(c)). Since the (sub)grid resulting from this partition has more columns than rows, it is vertically split. Again, each resulting partition receives half of the columns (6). The top-left corner cell of the resulting grid from the left partition receives the index $(0, 0)$, whereas the top-left corner cell of the resulting grid from the right partition receives the index $(0, 6)$. This partitioning process is then recursively applied to the resulting partitions (Fig. 3(d)) until each partition contains only one point.

Algorithm 2 puts all these pieces together. Function $\text{SPLIT}_y(\mathcal{C}, K)$ performs the horizontal bisection. In this process, \mathcal{C} is sorted according to the y -coordinates (\mathcal{C} is viewed as a list). The first K instances are assigned to \mathcal{C}_1 and the remaining to \mathcal{C}_2 . The function $\text{SPLIT}_x(\mathcal{C}, K)$ performs the vertical bisection using the same process, but sorting \mathcal{C} according to the x -coordinates. Notice that, from an implementation perspective, we use a pre-sorting strategy [5] so that the x - and y -

coordinates are only sorted once. Although we have discussed our process as a grid index assignment, the depicted algorithm already transforms such indexes into coordinates.

Algorithm 2 Assigning points to grid cell positions.

Input:

$\mathcal{C} = \mathcal{P} \cup \mathcal{D}$ \triangleright Scatterplot with “dummy” and original points
 R, C \triangleright Grid dimensions (rows and columns)
 w_{\max}, h_{\max} \triangleright Max marker width/height in \mathcal{P}

Output:

$\mathcal{P}' = \{p'_1, \dots, p'_N\}$ \triangleright Transformed points

function DGRID($\mathcal{C}, (R, C)$)
 DGRID_AUX($\mathcal{C}, (R, C), (0, 0)$)
 return \mathcal{P}'
end function

function DGRID_AUX($\mathcal{C}, (R, C), (i, j)$)
 if $\mathcal{C} \neq \emptyset$ **then**
 if $|\mathcal{C}| = 1$ **then** $\triangleright \mathcal{C}$ has one point
 if $c \in \mathcal{C}$ is a original point **then**
 $\mathcal{P}' \leftarrow \mathcal{P}' \cup \{j \times w_{\max}, i \times h_{\max}\}$
 end if
 else
 if $R > C$ **then**
 $\mathcal{C}_1, \mathcal{C}_2 \leftarrow \text{SPLIT}_y(\mathcal{C}, \min(|\mathcal{C}|, \lceil R/2 \rceil \times C))$
 DGRID_AUX($\mathcal{C}_1, (\lceil R/2 \rceil, C), (i, j)$)
 DGRID_AUX($\mathcal{C}_2, (R - \lceil R/2 \rceil, C), (i + \lceil R/2 \rceil, j)$)
 else
 $\mathcal{C}_1, \mathcal{C}_2 \leftarrow \text{SPLIT}_x(\mathcal{C}, \min(|\mathcal{C}|, R \times \lceil C/2 \rceil))$
 DGRID_AUX($\mathcal{C}_1, (R, \lceil C/2 \rceil), (i, j)$)
 DGRID_AUX($\mathcal{C}_2, (R, C - \lceil C/2 \rceil), (i, j + \lceil C/2 \rceil)$)
 end if
 end if
 end if
end function

Notice that, since each original and “dummy” point is assigned to an individual cell, and we have the same number of points and cells, the result is a complete overlap-free representation (**DG1**).

3.2.4 Computational Complexity

To set DGrid’s computational complexity, we first split the suggested process into two major phases, “dummy” points creation and grid assignment. Considering $T = R \times C > N$ the total number of grid cells, the complexity of creating the “dummy” points is $O(T \log T)$ if a nearest neighbor data structure is used to find the nearest neighbors, such as a k -d tree [2], and a $O(n \log n)$ sorting algorithm is applied to define the final list of points (FILTER() function). For the second phase, if an $O(n \log n)$ algorithm is also used to sort the points’ x - and y -coordinates, its computational complexity is $O(T \log T)$. Assuming that the original scatterplot occupies a finite area and that the ratio between this area and the summation of all markers area is bounded by a small constant (see Eq. (9)), DGrid’s overall complexity is $O(N \log N)$.

4 RESULTS

In this section, we quantitatively evaluate and compare DGrid against the state-of-the-art, present two different use-cases to highlight the advantages of using an overlap-free layout if compared to traditional DR layouts, and finish with a user evaluation to measure subjective elements that are not possible to capture through quality metrics.

4.1 Evaluation and Comparison

For the quantitative evaluation, we compare DGrid against ReArrange, PFS’, VPSC, RWordle-L, RWordle-C, ProjSnippet, and PRISM (see Sec. 2) techniques. In this comparison, we use the 7 different quality metrics defined in Sec. 3.1 aiming at assessing the structure preservation of the resulting overlap-free scatterplots.

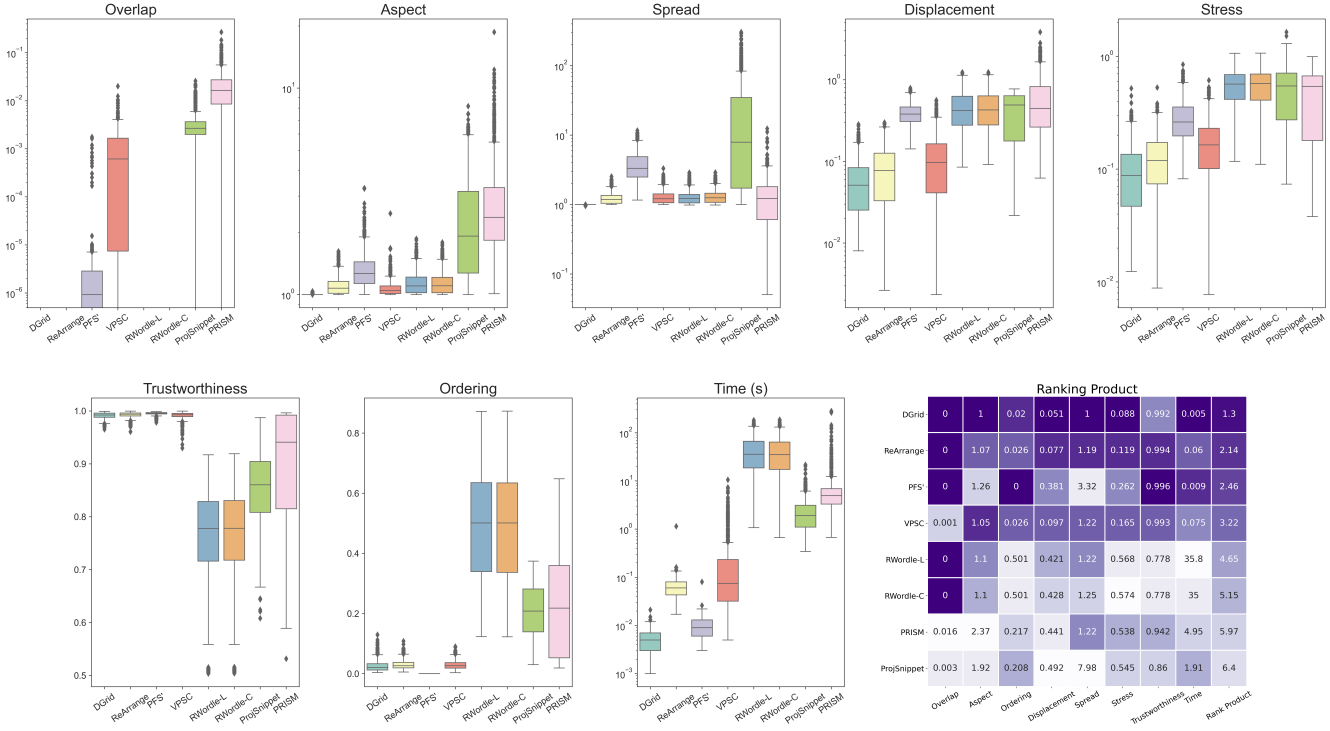


Fig. 4. Boxplots summarizing the results of each technique considering the different metrics defined in Sec. 3.1 and the running-time. A Ranking Product matrix is also presented aggregating all the results to rank the techniques according to their median results. The cells' values are the median, and the darker the cell, the better the ranking position. Considering the combination of all these metrics, DGrid is the top-ranked technique.

For the tests, we generate 1,000 different scatterplots varying the sizes between 500 and 1,000 points, the densities, that is, the ratio between the scatterplot area and markers' area (see Eq.(9)) in [3, 5, 7, 9, 11], the aspect-ratios between [1, 4], and the number of groups in [1, 2, 3, 4, 5] considering different Gaussian distributions, controlling the overlap level in each group (from very dense to sparse groups). We prefer to use synthetic scatterplots since this allows us to better control the experiments, producing layouts with varying aspects and helping to uncover the reasons for the attained results. All the results were generated in an Intel(R) Core(TM) i7-8700 CPU @ 3.20 GHz, 32 GB RAM, Ubuntu 64 bits, NVIDIA GeForce GTX 1660 Ti 22 GB. The techniques were implemented in Java. For the ReArrange, RWordle-L, and RWordle-C, we used the authors' original codes. The others we implemented. All the produced code and datasets are available at [removed_for_reviewing].

Our analysis is presented in Figs. 4 and 5. Fig. 4 presents boxplots summarizing the results of each technique considering the different metrics. Fig. 5 presents heatmaps with correlations between these metrics and the original scatterplots densities (Eq. 9) and overlap coefficients (Eq. 1). We use this correlation analysis to understand, per technique, how the different characteristics of the original scatterplots may affect the quality of the produced overlap-free layouts. In the heatmaps, we only show cells with statistical significance ($p < 0.01$).

Interestingly, PFS', VPSC, ProjSnippet, and PRISM were not able to entirely remove overlaps (Fig. 4). The problems of ProjSnippet and PRISM have roots in the employed optimization process and numerical stability. We tried to use gradient clipping to alleviate them, especially the exploding gradient issue (not mentioned in the original papers), but with limited success. For the PFS' and VPSC, we cannot fully understand the causes, but we know that the resulting overlap is positively correlated with the original scatterplots overlap (Fig. 5). That is, as the original overlap increases, the final overlap also increases. Notice that this is also true for the ProjSnippet and PRISM, with a fascinating negative correlation for ProjSnippet (no clues why). For both techniques, the negative result in overlap removal is also correlated

with the original scatterplots' density, meaning that these techniques do not work properly when the original scatterplot is severely cluttered. DGrid, ReArrange, RWordle-L, and RWordle-C, completely removed the overlaps in all scenarios.

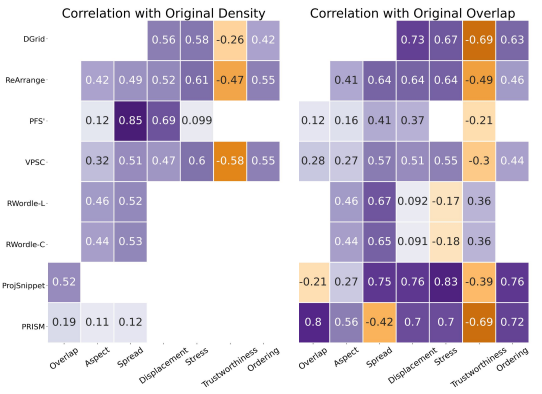


Fig. 5. Correlation heatmaps showing how the densities and overlap coefficients of original scatterplots may influence, per technique, the quality of the produced layouts. The missing cells are correlations without statistical significance.

In terms of aspect-ratio preservation (Fig. 4), DGrid is the only technique to reach a nearly optimum result, meaning that it is the only technique that can preserve original scatterplots' global shapes, while PFS', ProjSnippet, and PRISM present the most significant deformation. Checking the heatmaps (Fig. 5), it is possible to see that DGrid is the only technique that is not affected either by the original density or the original overlap. Similar results are presented for the spread. DGrid offers a nearly perfect spread, meaning it is the only one that preserves original marker sizes. PFS' and ProjSnippet present the most significant

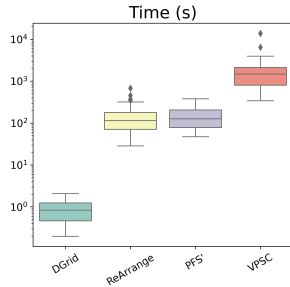


Fig. 6. Boxplot summarizing the results considering larger datasets (50k ~ 100K instances). Compared to the four fastest techniques, DGrid is two or three orders of magnitude faster.

spread, and PRISM often reduces the scatterplot area’s size. For most techniques, the spread is related to original density and overlap (since there is no variance on DGrid results, there is no correlation). This is not surprising since we intentionally preserve the original aspect-ratio and control the displacement by defining our grid dimensions according to the original scatterplot and using it as a constraint to moving points. The other techniques do not set these as hard restrictions, probably not to affect other metrics. Notice that, even with gradient clipping, PRISM could not create bounded overlap-free scatterplots for two scenarios. So we removed them from PRISM analysis.

Displacement and stress present similar results. DGrid renders the best result, closely followed by ReArrange and VPSC. PFS’ presents intermediate results and the others are on the same level of low distance preservation and high displacement. Therefore, DGrid, ReArrange, and VPSC maintain the original scatterplot’s general appearance, with low displacement and good global preservation of original distances. Locally, DGrid, ReArrange, PFS’, and VPSC present practically the same results regarding trustworthiness, with PFS’ attaining the best result. Not only do these techniques present the best results, but also the deviation is minimal. This indicates that neighborhoods are reliable, a fundamental characteristic since several analytical tasks executed using dimensionality reduction scatterplots are based on neighborhood analysis. Notice that it is necessary to establish the neighborhood size to calculate trustworthiness. Here we use the common heuristic of setting it to 5% of the scatterplot size.

For the last metric, orthogonal ordering, PFS’ renders the perfect result, with DGrid, ReArrange, and VPSC close by. These techniques have the lowest impact on the user’s mental map, meaning that if the user puts side-by-side the original and the transformed layout and focuses the analysis on one point, what is at the top/bottom, left/right of that point is preserved. However, for most techniques, there is a cost for that, which is an increased spread. ReArrange and VPSC increase the scatterplot sizes by 20% while the PFS’ increases more than 330%. DGrid ensures good orthogonal ordering without incurring in expanding the scatterplot area, preserving the perceived markers’ sizes.

In terms of running times, even though the datasets are small, two groups of techniques can be observed: one containing techniques that run under a second; and another composed of methods that need more (for some, much more) than that. DGrid is the fastest technique, with ReArrange, PFS’ and VPSC practically presenting the same execution time (the difference is in milliseconds). To show the real differences between these four faster techniques, we create 120 datasets following the same procedure explained before, but with sizes varying between 50,000 and 100,000. Fig. 6 presents the boxplot summarizing the results. DGrid (median=0.83s) is at least two orders of magnitude faster than the ReArrange (median=114.89s) and PFS’ (median=126.91s) and three orders faster than VPSC (median=1,471.35s).

Finally, we calculate the rank product [4] using all metrics and running-time (for the small datasets) to summarize these results. Rank product is a non-parametric statistical method used in biology to combine different ranks and define a general rank. If $r_{t,i}$ denotes the rank

position of technique t in the i^{th} metric, the final rank of t considering K different metrics is calculated as $(\prod_{i=1}^K r_{t,i})^{1/K}$. In our case, for each metric, we create a rank based on the techniques’ median values (rounding to the 3rd decimal place). Fig. 4 presents a heatmap showing the median results of each technique for each metric, with the cells colored according to the rank position per metric. The darker the color, the best the rank position. DGrid presents the best trade-off between all the techniques and is ranked the first in terms of attending the design guidelines presented in Sec. 3.1. ReArrange and PFS’ are in second place, with ReArrange presenting superior results. VPSC appears in the fourth position, RWordle-L in the fifth, RWordle-C and PRISM in the sixth, and ProjSnippet in the last, rendering DGrid a precise and fast approach to remove overlaps.

4.2 Use-Cases

To illustrate the benefits of using overlap-free layouts produced by DGrid, we present two different use-cases. We start with an exploratory analysis of the World Happiness Report 2019 [21] dataset¹. This dataset presents a ranking of 156 countries based on an index representing how happy their citizens perceive themselves, and other six variables to support the explanation of the happiness index variation across countries, including GDP per capita, social support, healthy life expectancy, freedom to make life choices, generosity, and perception of corruption.

Fig. 7 presents a UMAP [27] layout considering the six variables used to explain the happiness index (a high-resolution version of this image is included in the supplemental material). The visual markers encode the happiness index as horizontal black bars and other variables using bar charts to enrich our layout. In this layout, three different groups of countries are noticeable, and some instances of each group are visible (depending on the rendering order). Other than that, it is not easy to extract any other information without any auxiliary strategy, even for this considerably small dataset. Fig. 1 presents the same projection after DGrid rearranges the layout to remove overlaps. Even after reducing empty space, the three different groups are still readily noticeable. However, many other details are visible. The three groups represent different levels of happiness, from high in the top-left to low in the bottom-right. With the general magnitude of the variables following the same pattern, although it is possible to see that the three groups are not uniform (we use Euclidean distance, so this is expected, nevertheless, not easily seen in the original projection). Also, generosity (orange bar) varies without following the happiness pattern. Happiness and generosity do not walk together (which is confirmed by the correlation between the happiness index and generosity). Many other exciting findings can be extracted from this layout, only made possible by using more informative markers and removing the overlaps, leveraging projection to be valuable beyond clustering/segmentation tasks, opening the “black-box” of intra-group analysis.

The second use-case discusses how DGrid can improve Convolutional Neural Networks’ analysis (CNN) based on dimensionality reduction layouts. In this example, we project 3,000 images randomly selected from the Fashion MNIST [51] dataset using the dense layer as features. The network we use has two convolutional layers, followed by a dense layer with 128 neurons, followed by a softmax layer with 10 neurons. Fig. 8(A) shows the original UMAP projection. Markers’ colors indicate the ground truth labels of these images. Although it is possible to see how the different groups of images are similar, class-outlier analysis is challenging to execute. The class-outlier analysis is an essential task in classification models and focuses on assessing instances of a given class (colors in this example) inside a homogenous group of another class [41]. Fig. 8(B) presents the result of using DGrid in this layout. As in the first use-case, the inter-group relationships are maintained, but, since in this example, the proportional available space is larger, the groups’ shapes are well preserved and compared to the original layout, the outliers are easier to spot. For instance, the three outliers in the blue group in the top-right are now visible. Also, class

¹<https://www.kaggle.com/unsdsn/world-happiness>

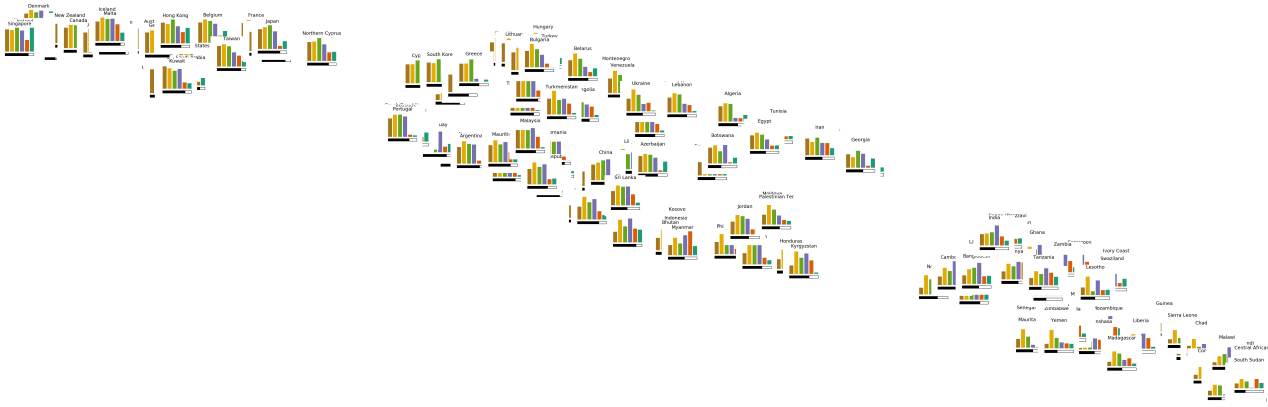


Fig. 7. DR layout of the happiness index dataset. Bar charts are used to enhance the exploratory analysis showing the different variables in this dataset. Even for a small dataset, overlaps affect intra-group analysis and a detail view of the individual instances.

purity is easier to infer. For instance, the blue group (top-right) is purer than the light blue group (middle-right).

Fig. 8(C) shows an enlargement of the purple group using the original images as an alternative marker. It is now possible to see that not only the CNN separates well this group of images (purses) from the others, but also this group present an internal organization. There is a tendency to separate purses with visible handles (right side) from purses without (left side) and the presence of some miss-classified instances, indicated by the image borders colored with the ground truth color. To help understand why the CNN has confused those images with purses, we use SHAP [24] to explain which part of the images contribute to the confusion. Fig. 8(D) shows the contribution of different parts of one miss-classified image (a dress) to increase (in red) or to decrease (in blue) the probability of being classified in every class. The selected image was misclassified as a purse due to its format and color intensity (see the SHAP values for the image inside the dashed square). For instance, the top part of the dress was probably misunderstood as a handle. This fact is testified by the explanations of neighborhood images, in which the rectangular shape and visible handles contribute to augment the probability of that class.

4.3 User Evaluation

Some characteristics of the technique, such as the produced layouts' general appearance, are inherently subjective and much harder to capture with objective metrics. For example, since we use orthogonal partitioning in the grid assignment process, high-dense groups, especially those close to the scatterplot borders, tend to have rectangular sides or shapes. Also, the points are aligned into a grid, which interferes with their free distribution but may lead to a more organized look and feel. To account for these aspects, we executed a user test to evaluate how this impacts user perception of the preservation of patterns and the aesthetics of the produced layouts.

The test consisted of two main parts. In the first part, given an original scatterplot (with overlap) and eight possible overlap-free alternatives produced by different techniques, the participant was asked to select a minimum of one and a maximum of three overlap-free layouts that best preserved the general characteristics (patterns) of the original, e.g., general scatterplot format (width/height), groups, borders between groups, item positions, and item size. In the second part, given eight overlap-free alternatives produced by different techniques (without the original), the participant was asked to choose the one that is the most aesthetically pleasing and easy to understand (regarding, e.g., separation and boundaries between groups). Each participant assessed 15 sets of scatterplots in the first part (*patterns*) and 10 sets in the second part (*aesthetics*). The scatterplots were anonymized (i.e., the participant did not know which technique generated them), and the presentation order of the eight alternatives was always randomized per set and participant. The test was distributed online via Google Forms and was performed

by 42 volunteers from various universities in different countries and continents (more information about the participants can be found in the supplemental material).

The results—the distributions of scores for each technique in both parts of the user evaluation—are shown in Fig. 9. In the first part, we compute a score for each technique (per participant) as follows. Every time a technique is selected as one of the best overlap-free alternatives, it receives a score of $1/N_{choices}$, where $N_{choices} \in \{1, 2, 3\}$ is the number of alternatives selected for the same set. Thus, if the participant selected only one alternative, it gets the maximum score of 1 for that specific set; otherwise, it gets a score of either $\frac{1}{2}$ or $\frac{1}{3}$. The final score of that participant's technique is the sum of the scores for all the 15 assessed sets of scatterplots. In the second part, each technique's score (per participant) is simply the number of times it was selected as the most aesthetic-pleasing alternative.

DGrid achieves the highest average scores (M) in both parts of the evaluation : ($M = 5.329, SD = 3.060$) for the first (*patterns*), and ($M = 5.166, SD = 4.131$) for the second (*aesthetics*). The second-highest scores come from ReArrange in both cases: ($M = 3.805, SD = 1.797$) for the first part of the test, and ($M = 2.928, SD = 3.063$) for the second. Due to the considerable amount of variability in the results, we further tested DGrid's scores against ReArrange using two one-tailed two-sample t -tests, one for each part. Our null hypotheses are that DGrid's scores are statistically the same as ReArrange's, while our alternative hypotheses are that they are higher (with $\alpha = 0.1$). The results are significant in both cases, with $p = .003351$ for the first part (*patterns*) and $p = .00301$ for the second (*aesthetics*). Thus, we rejected both null hypotheses in favor of the alternative ones.

5 DISCUSSIONS AND LIMITATIONS

In our solution for assigning points to a grid (Algorithm 2), the splitting process uses a simple heuristic to partition the points, splitting them into sub-partitions with similar sizes. An alternative to improve could be to use a strategy to find the best (orthogonal) partitioning, for instance, the Jenks' Natural Break [22]. The Natural Break is a clustering approach that partitions univariate datasets to reduce the variance within-cluster and maximize the variance between clusters. We have tested with that, and the marginal improvement does not justify the increase in complexity and running time. We input two main reasons for this result. First, considering a bisection to produce a (sub)grid with R rows and C columns, we have only $R - 1$ possible horizontal cuts and $C - 1$ possible vertical cuts. So, there is no much room for defining the best partition. Second, since the “dummy” points are distributed following the grid cells, the regions of empty spaces present perfect uniform marginal distributions, so a different splitting does not change the outcome. Another design consideration is why not fixing the “dummy” points and moving only the original points? Although a reasonable idea, fixing “dummy” points do not work in practice. Since the process to

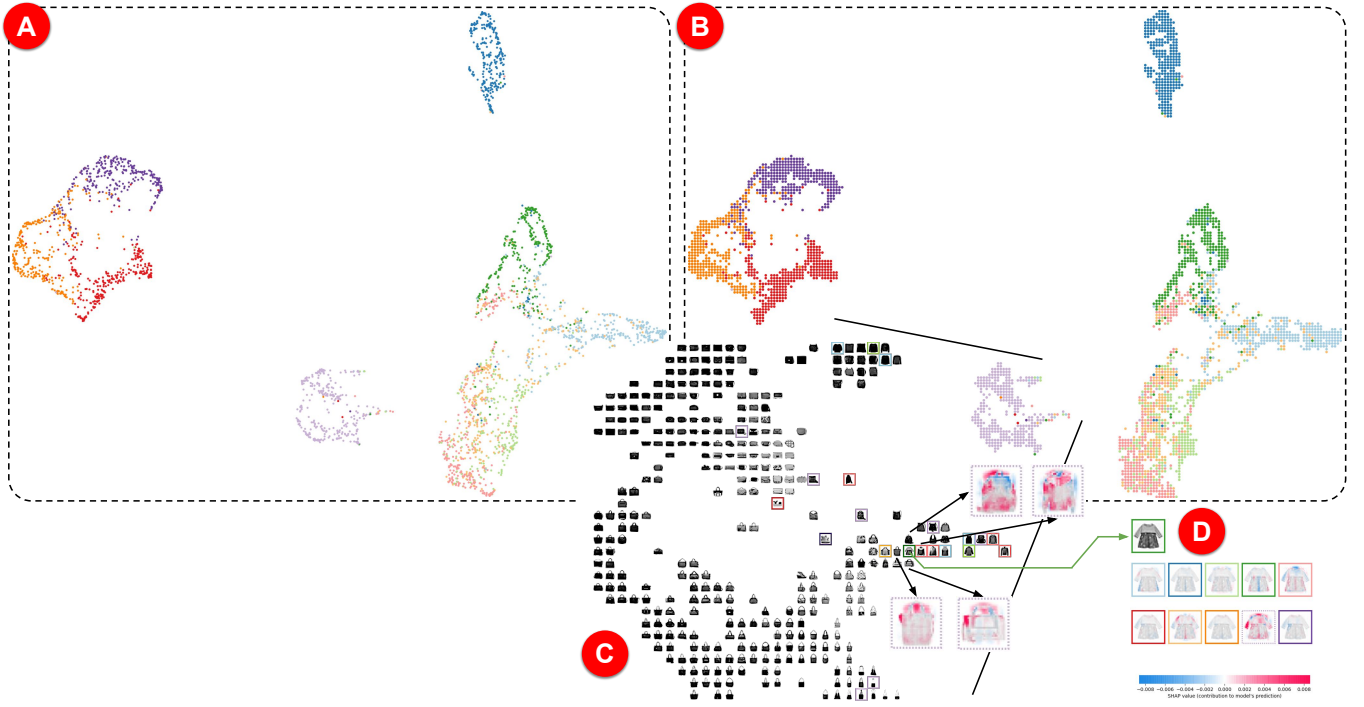


Fig. 8. Using dimensionality reduction and DGrid to analyze CNN results. The original layout is produced using UMAP, and the instances are colored according to ground truth (A). After applying DGrid to remove overlaps, the general appearance is maintained, but class-outliers are easier to spot (B). One group is zoom in for analysis, and images are used as markers, allowing the visualization of intra-group patterns (C). To further investigate misclassifications, SHAP is used to show which part of the images contributes to the mistakes (D).

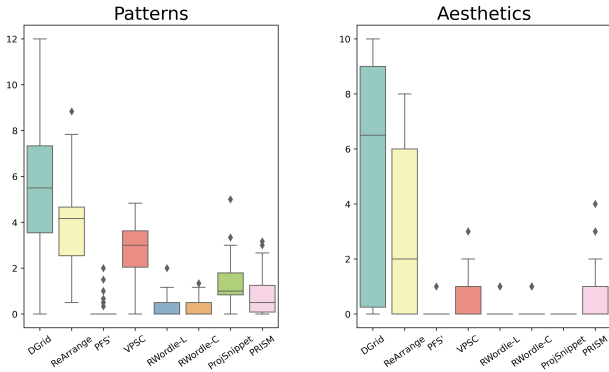


Fig. 9. Results of the user evaluation. DGrid has the highest average scores for both patterns and aesthetics.

create such points does not guarantee that the number of not occupied cells close to a high-density region is equal to the number of original points in that region, original points can be drastically displaced if the “dummy” points do not move.

Overlap in scatterplots is a well-documented problem [43, 44], and apparently, overlap removal can be the holy grail. However, this is not true in some cases and for some tasks. Firstly, removing overlaps affects distribution detection tasks. This is true for all techniques that limit the visual area to keep markers at a readable size. A simple solution could be to show side-by-side the original and the overlap-free scatterplots. In this case, a precise technique, such as DGrid or ReArrange, is mandatory, so the user’s mental map is preserved between visualizations. Secondly, the visual area where the overlap free scatterplot is rendered needs to allow the removal. It is possible to remove overlaps only if the proportion between the available space and total

markers area is larger than one (see Eq. 9). Indeed, if this proportion is not significant and the original scatterplot presents high-density regions, the produced scatterplot will merge groups, impacting class separation tasks [31]. This is also valid for all overlap removal techniques. One solution is to increase the available space, but incurring in reducing markers size. Another is to use a sampling technique [52] before removing the overlaps. In any case, users should carefully consider the tradeoff between space preservation and markers’ dimensions, and a fast technique like DGrid makes testing multiple solutions, even for large datasets, an inexpensive task.

Finally, DGrid allocates the same layout area to each marker. Although markers’ dimensions can vary inside that area, if they are too discrepant, unnecessary space may be added to the overlap-free layout, even potentially creating artifacts in the final visualization. Although the resulting alignment showed beneficial, bringing some organization to the visualization (one of the main principles in interface design), other solutions for removing overlap are preferable if markers with significantly varying dimensions are required.

6 CONCLUSIONS

In this paper, we proposed *Distance-preserving Grid (DGrid)*, a novel approach for overlap removal of Dimensionality Reduction (DR) layouts. DGrid is a two-step approach that completely removes overlap and maintains original scatterplot aspect ratio and markers’ sizes while preserves distance and neighborhood relationships, an essential feature for DR layouts. The set of comparisons we provide shows that DGrid outperforms the existing state-of-the-art techniques considering different quality metrics and is two to three orders of magnitude faster than the fastest existing techniques. A user test attests the good results, with most participants selecting DGrid layouts as ones that best preserve original patterns and are aesthetically pleasing. The quality of the produced layouts combined with the low computational cost render DGrid one of the most attractive methods to date, allowing inter-group and class-outlier analyses that are usually challenging in typical DR layouts.

REFERENCES

- [1] J. A. Anderson and E. Rosenfeld, eds. *Neurocomputing: Foundations of Research*. MIT Press, Cambridge, MA, USA, 1988.
- [2] J. L. Bentley. Multidimensional binary search trees used for associative searching. *Commun. ACM*, 18(9):509–517, Sept. 1975.
- [3] R. Brath. 3d infovis is here to stay: Deal with it. In *2014 IEEE VIS International Workshop on 3DVis (3DVis)*, pp. 25–31, 2014. doi: 10.1109/3DVis.2014.7160096
- [4] R. Breitling, P. Armengaud, A. Amtmann, and P. Herzyk. Rank products: a simple, yet powerful, new method to detect differentially regulated genes in replicated microarray experiments. *FEBS Letters*, 573(1-3):83–92, 2004. doi: 10.1016/j.febslet.2004.07.055
- [5] R. A. Brown. Building a balanced k -d tree in $o(kn \log n)$ time. *Journal of Computer Graphics Techniques (JCGT)*, 4(1):50–68, March 2015.
- [6] N. Cao, D. Gotz, J. Sun, and H. Qu. Dicon: Interactive visual analysis of multidimensional clusters. *IEEE Transactions on Visualization and Computer Graphics*, 17(12):2581–2590, 2011. doi: 10.1109/TVCG.2011.188
- [7] D. B. Carr, R. J. Littlefield, W. L. Nicholson, and J. S. Littlefield. Scatterplot matrix techniques for large n . *Journal of the American Statistical Association*, 82(398):424–436, 1987. doi: 10.1080/01621459.1987.10478445
- [8] F. Chen, L. Piccinini, P. Poncelet, and A. Sallaberry. Node overlap removal algorithms: an extended comparative study. *Journal of Graph Algorithms and Applications*, 24(4):683–706, 2020. doi: 10.7155/jgaa.00532
- [9] F. Chen, L. Piccinini, P. Poncelet, and A. Sallaberry. Node overlap removal algorithms: an extended comparative study. *Journal of Graph Algorithms and Applications*, 24(4):683–706, 2020. doi: 10.7155/jgaa.00532
- [10] F. S. L. G. Duarte, F. Sikansi, F. M. Fatore, S. G. Fadel, and F. V. Paulovich. Nmap: A novel neighborhood preservation space-filling algorithm. *IEEE Transactions on Visualization and Computer Graphics*, 20(12):2063–2071, 2014. doi: 10.1109/TVCG.2014.2346276
- [11] T. Dwyer, K. Marriott, and P. J. Stuckey. Fast node overlap removal. In P. Healy and N. S. Nikolov, eds., *Graph Drawing*, pp. 153–164. Springer Berlin Heidelberg, Berlin, Heidelberg, 2006.
- [12] D. M. Eler, M. V. Nakazaki, F. V. Paulovich, D. P. Santos, G. de Faria Andery, M. C. F. de Oliveira, J. B. Neto, and R. Minghim. Visual analysis of image collections. *Vis. Comput.*, 25(10):923–937, 2009. doi: 10.1007/s00371-009-0368-7
- [13] N. Elmqvist. Balloonprobe: Reducing occlusion in 3d using interactive space distortion. In *Proceedings of the ACM Symposium on Virtual Reality Software and Technology*, VRST '05, p. 134–137. Association for Computing Machinery, New York, NY, USA, 2005. doi: 10.1145/1101616.1101643
- [14] D. Eppstein, M. van Kreveld, B. Speckmann, and F. Staals. Improved grid map layout by point set matching. In *2013 IEEE Pacific Visualization Symposium (PacificVis)*, pp. 25–32, 2013. doi: 10.1109/PacificVis.2013.6596124
- [15] O. Fried, S. DiVerdi, M. Halber, E. Sizikova, and A. Finkelstein. Isomatch: Creating informative grid layouts. *Comput. Graph. Forum*, 34(2):155–166, May 2015.
- [16] E. Gansner and Y. Hu. Efficient, proximity-preserving node overlap removal. *J. Graph Algorithms Appl.*, 14:53–74, 2010.
- [17] M. v. Garderen, B. Pampel, A. Nocaj, and U. Brandes. Minimum-Displacement Overlap Removal for Geo-referenced Data Visualization. *Computer Graphics Forum*, 2017. doi: 10.1111/cgf.13199
- [18] E. Gomez-Nieto, W. Casaca, L. G. Nonato, and G. Taubin. Mixed integer optimization for layout arrangement. In *2013 XXVI Conference on Graphics, Patterns and Images*, pp. 115–122, 2013. doi: 10.1109/SIBGRAPI.2013.25
- [19] E. Gomez-Nieto, F. S. Roman, P. Pagliosa, W. Casaca, E. S. Helou, M. C. F. de Oliveira, and L. G. Nonato. Similarity preserving snippet-based visualization of web search results. *IEEE Transactions on Visualization and Computer Graphics*, 20(3):457–470, 2014. doi: 10.1109/TVCG.2013.242
- [20] K. Hayashi, M. Inoue, T. Masuzawa, and H. Fujiwara. A layout adjustment problem for disjoint rectangles preserving orthogonal order. In *Graph Drawing*, 1998.
- [21] J. Helliwell, R. Layard, and J. Sachs. *World Happiness Report 2019*. New York: Sustainable Development Solutions Network, 2019.
- [22] G. F. Jenks. The data model concept in statistical mapping. *International Yearbook of Cartography*, 7:186–190, 1967.
- [23] J. Kruskal. Multidimensional scaling by optimizing goodness of fit to a nonmetric hypothesis. *Psychometrika*, 29(1):1–27, 1964.
- [24] S. M. Lundberg and S.-I. Lee. A unified approach to interpreting model predictions. In I. Guyon, U. V. Luxburg, S. Bengio, H. Wallach, R. Fergus, S. Vishwanathan, and R. Garnett, eds., *Advances in Neural Information Processing Systems 30*, pp. 4765–4774. Curran Associates, Inc., 2017.
- [25] W. E. Marcilio-Jr, D. M. Eler, R. E. Garcia, and I. R. V. Pola. Evaluation of approaches proposed to avoid overlap of markers in visualizations based on multidimensional projection techniques. *Information Visualization*, 18(4):426–438, 2019. doi: 10.1177/1473871619845093
- [26] A. Mayorga and M. Gleicher. Splatterplots: Overcoming overdraw in scatter plots. *IEEE Transactions on Visualization and Computer Graphics*, 19(9):1526–1538, 2013. doi: 10.1109/TVCG.2013.65
- [27] L. McInnes, J. Healy, and J. Melville. Umap: Uniform manifold approximation and projection for dimension reduction, 2020.
- [28] G. McNeill and S. A. Hale. Generating tile maps. *Computer Graphics Forum*, 36(3):435–445, 2017. doi: 10.1111/cgf.13200
- [29] W. Meulemans. Efficient optimal overlap removal: Algorithms and experiments. *Computer Graphics Forum*, 38(3):713–723, 2019. doi: 10.1111/cgf.13722
- [30] W. Meulemans, J. Dykes, A. Slingsby, C. Turkay, and J. Wood. Small multiples with gaps. *IEEE Transactions on Visualization and Computer Graphics*, 23(1):381–390, Jan 2017.
- [31] L. Micallef, G. Palmas, A. Oulasvirta, and T. Weinkauff. Towards perceptual optimization of the visual design of scatterplots. *IEEE Transactions on Visualization and Computer Graphics*, 23(6):1588–1599, 2017. doi: 10.1109/TVCG.2017.2674978
- [32] K. Misue, P. Eades, W. Lai, and K. Sugiyama. Layout adjustment and the mental map. *J. Vis. Lang. Comput.*, 6:183–210, 1995.
- [33] K. Misue, P. Eades, W. Lai, and K. Sugiyama. Layout adjustment and the mental map. *Journal of Visual Languages & Computing*, 6(2):183–210, 1995. doi: 10.1006/jvlc.1995.1010
- [34] L. Nachmanson, A. Nocaj, S. Bereg, L. Zhang, and A. Holroyd. Node overlap removal by growing a tree. In Y. Hu and M. Nöllenburg, eds., *Graph Drawing and Network Visualization*, pp. 33–43. Springer International Publishing, Cham, 2016.
- [35] L. G. Nonato and M. Aupetit. Multidimensional projection for visual analytics: Linking techniques with distortions, tasks, and layout enrichment. *IEEE Transactions on Visualization and Computer Graphics*, 25(8):2650–2673, 2019. doi: 10.1109/TVCG.2018.2846735
- [36] R. Pinho and M. C. F. de Oliveira. Hexboard: Conveying pairwise similarity in an incremental visualization space. In *2009 13th International Conference Information Visualisation*, pp. 32–37, 2009. doi: 10.1109/IV.2009.12
- [37] R. Pinho, M. C. F. de Oliveira, and A. de A. Lopes. Incremental board: A grid-based space for visualizing dynamic data sets. In *Proceedings of the 2009 ACM Symposium on Applied Computing*, p. 1757–1764. Association for Computing Machinery, New York, NY, USA, 2009. doi: 10.1145/1529282.1529679
- [38] N. Quadrianto, L. Song, and A. Smola. Kernelized sorting. *IEEE Transactions on Pattern Analysis and Machine Intelligence*, 32:1809–1821, 2010.
- [39] E. Raisz. The rectangular statistical cartogram. *Geographical Review*, 24:292–296, 1934.
- [40] A. B. Ramos-Guajardo, G. González-Rodríguez, and A. Colubi. Testing the degree of overlap for the expected value of random intervals. *International Journal of Approximate Reasoning*, 119:1–19, 2020. doi: 10.1016/j.ijar.2019.12.012
- [41] P. E. Rauber, A. X. Falcão, and A. C. Telea. Projections as visual aids for classification system design. *Information Visualization*, 17(4):282–305, 2018. doi: 10.1177/1473871617713337
- [42] D. Sacha, L. Zhang, M. Sedlmair, J. A. Lee, J. Peltonen, D. Weiskopf, S. C. North, and D. A. Keim. Visual interaction with dimensionality reduction: A structured literature analysis. *IEEE Transactions on Visualization and Computer Graphics*, 23(1):241–250, 2017. doi: 10.1109/TVCG.2016.2598495
- [43] A. Sarikaya and M. Gleicher. Scatterplots: Tasks, data, and designs. *IEEE Transactions on Visualization and Computer Graphics*, 24(1):402–412, 2018. doi: 10.1109/TVCG.2017.2744184
- [44] M. Sedlmair, T. Munzner, and M. Tory. Empirical guidance on scatterplot and dimension reduction technique choices. *IEEE Transactions on Visualization and Computer Graphics*, 19(12):2634–2643, 2013. doi: 10.1109/TVCG.2013.153
- [45] H. Strobel, M. Spicker, A. Stoffel, D. Keim, and O. Deussen. Rolled-out

wordles: A heuristic method for overlap removal of 2d data representatives. *Computer Graphics Forum*, 31, 2012.

- [46] G. Strong and M. Gong. Data organization and visualization using self-sorting map. In *Proceedings of Graphics Interface 2011*, GI '11, p. 199–206, 2011.
- [47] M. van Kreveld and B. Speckmann. On rectangular cartograms. In S. Albers and T. Radzik, eds., *Algorithms – ESA 2004*, pp. 724–735. Springer Berlin Heidelberg, Berlin, Heidelberg, 2004.
- [48] J. Venna and S. Kaski. Neighborhood preservation in nonlinear projection methods: An experimental study. In G. Dorffner, H. Bischof, and K. Hornik, eds., *Artificial Neural Networks — ICANN 2001*, pp. 485–491. Springer Berlin Heidelberg, Berlin, Heidelberg, 2001.
- [49] J. Wood and J. Dykes. Spatially ordered treemaps. *IEEE Transactions on Visualization and Computer Graphics*, 14(6):1348–1355, 2008. doi: 10.1109/TVCG.2008.165
- [50] J. Wood, J. Dykes, and A. Slingsby. Visualisation of origins, destinations and flows with od maps. *The Cartographic Journal*, 47:117 – 129, 2010.
- [51] H. Xiao, K. Rasul, and R. Vollgraf. Fashion-mnist: a novel image dataset for benchmarking machine learning algorithms. *ArXiv*, abs/1708.07747, 2017.
- [52] J. Yuan, S. Xiang, J. Xia, L. Yu, and S. Liu. Evaluation of sampling methods for scatterplots. *IEEE Transactions on Visualization and Computer Graphics*, 27(02):1720–1730, feb 2021. doi: 10.1109/TVCG.2020.3030432